Cite this: *J. Mater. Chem. B*, 2019, **7**, 1116

Perfluorocarbon-based O_2 nanocarrier for efficient photodynamic therapy†

Huamin Hu, ‡[a] Xuefeng Yan,‡[b] Hui Wang,[b] Joji Tanaka,[a] Mengzhe Wang,[b] Wei You *[a] and Zibo Li *[b]

Received 15th July 2018,
Accepted 14th January 2019

DOI: 10.1039/c8tb01844h

rsc.li/materials-b

Tumor hypoxia is considered as one of the major factors that limit the efficiency of photodynamic therapy (PDT), in which oxygen (O_2) is needed to generate singlet oxygen ($^1O_2$) for cell destruction. Inspired by the excellent O_2 carrying ability of perfluorocarbon molecules in artificial blood, we prepared a series of polymer micelles with a perfluorocarbon core to carry both photo-sensitizer and O_2 to the tumor site, aiming to improve PDT efficiency. We found that the accelerated generation of $^1O_2$ correlated with the increased perfluorocarbon amount in solution. *In vitro* cell study further showed that the new perfluorocarbon formulation not only improved the production of $^1O_2$, leading to enhanced photodynamic therapy efficiency, but also significantly reduced cell toxicity when compared with the one without these perfluoro units. This work provides a new option for improving PDT efficiency with the new perfluorocarbon-incorporated nanoplatform.

1. Introduction

Photodynamic therapy (PDT) is a clinically approved and minimally invasive treatment that can generate selective cytotoxic activity at tumor sites.[1] Typically, PDT relies on three main factors, namely, photosensitizer (PS) delivery, photon absorption, and tissue oxygen (O_2) supply. After irradiation at a specific wavelength, the PS absorbs the energy from a photon, followed by energy transfer to surrounding O_2 at the tumor site to generate cytotoxic singlet oxygen ($^1O_2$), which can trigger apoptotic and necrotic cell death.[2] Unfortunately, the effectiveness of PDT is often limited by inadequate oxygen at the tumor site (*i.e.*, hypoxia environment), which is exacerbated by the oxygen self-consuming mechanism of PDT. Therefore, overcoming the tumor hypoxia condition is crucial to improve the efficiency of PDT.[3]

To ensure the PDT efficacy, various nanomaterials have been developed to increase the O_2 concentration at the tumor site. The first approach is to produce O_2 directly at the tumor site, taking advantage of the endogenous hydrogen peroxide (H_2O_2) existing inside the tumor with a catalyst such as manganese dioxide (MnO_2) nanoparticles,[4,5] manganese ferrite nanoparticles ($MnFe_2O_4$),[6] or catalase,[7] to trigger the decomposition of H_2O_2 to produce O_2 *in situ*. However, this method cannot provide continuous production of O_2, again, due to the limited supply of H_2O_2 reactant available in the tumor microenvironment. Alternatively, several nanomaterials were reported to directly deliver natural O_2 to the tumor site.[8,9] For example, perfluorocarbons (PFCs, consisting of carbon chains with complete fluorination of the carbon skeleton) have excellent oxygen affinity due to the high electronegativity of the fluorine motif.[10] The chemically inert PFC often leads to good biocompatibility as well.[11,12] Because of their good oxygen carrying capability and excellent biocompatibility, small PFC molecules have been recently used to deliver O_2 to the tumor site.[13] Nonetheless, due to the immiscibility of PFC and H_2O, this method often requires the utilization of surfactants to form an emulsion[14] or human serum albumin (HSA)[15] protein for stabilization (Scheme 1). Moreover, similar to artificial blood, this method usually requires a high concentration of PFC – typically a minimal concentration around 20% w/v in water – in order to achieve good O_2 carrying ability.[13]

To simplify the composition of PFC-based emulsion, *e.g.*, eliminating the use of surfactants and/or other stabilizing reagent, yet still achieving high local concentration of PFC for O_2 carrying ability, polymer micelles with a PFC core have emerged as a promising approach (Scheme 1).[16] Furthermore, the hydrophobic photosensitizer (PS) can be embedded within these polymer micelle-based nanocarriers and delivered to the tumor site *via* the enhanced permeation and retention (EPR) effect.[17,18] One good example was recently presented by the Huang group.[19] The authors incorporated fluorinated segments (*i.e.*, pentafluorophenyl) into the core of the polymer micelle

[a] *Department of Chemistry, University of North Carolina at Chapel Hill, Chapel Hill, North Carolina 27599-3290, USA. E-mail: wyou@unc.edu*
[b] *Department of Radiology, University of North Carolina at Chapel Hill, Chapel Hill, North Carolina 27599, USA. E-mail: ziboli@med.unc.edu*

† Electronic supplementary information (ESI) available. See DOI: 10.1039/c8tb01844h

‡ These two authors contributed equally.

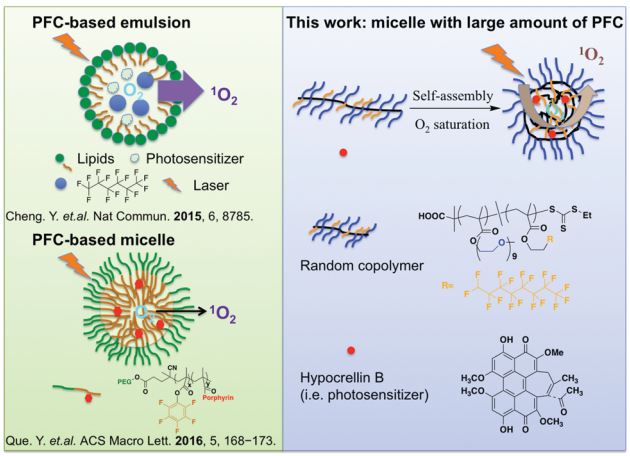

Scheme 1 Perfluorocarbon (PFC)-based O_2 delivery system for enhancing PDT efficiency.

nanocarrier in their study. These micelles with a fluorinated core are not only able to solubilize the PS but also able to significantly increase the local oxygen concentration surrounding PS and improve the efficacy of PDT. Unfortunately, in order to have a good solubility of these polymers, they were only able to incorporate a small amount of fluorine. Specifically, the concentration of micelles used for PDT was only around 0.1 mg mL^{-1}, which translated into a rather limited amount of fluorine in the solution (F amount in solution: 0.22 mM). Since the amount of perfluorocarbon motif directly affects the O_2 carrying capability and thereby the efficiency of PDT, polymers with significantly increased amounts of fluorine while still having good solubility under physiological conditions would be desirable.

Recently, the Maynard group reported amphiphilic/fluorous random copolymers as a new class of non-cytotoxic polymeric materials for biological applications, *e.g.*, protein conjugation.[20] Recognizing the fluorine-containing nature of these random copolymers, we envisioned to apply similar amphiphilic/fluorous random copolymers as O_2 carriers for PDT based on the following reasons. First, these amphiphilic random copolymers have good solubility; for instance, polymers with a concentration of 10 mg mL^{-1} (F amount in solution: 3.92 mM) can dissolve very well in H_2O.[20] Second, these amphiphilic/fluorous random copolymers can self-assemble into micelles in H_2O, which could embed the hydrophobic PS. Third, compared to block copolymers, random copolymers are also much easier to synthesize. In this work, we prepared a series of amphiphilic/fluorous random copolymers with different amounts of perfluorocarbon (*i.e.*, perfluorooctyl) through reversible addition–fragmentation chain transfer (RAFT) polymerization. Indeed, these polymers are able to self-assemble into micelles in H_2O, which agrees well with the previous report.[20] As expected, we find that the O_2 carrying ability is directly related to perfluorocarbon amount in solution. More importantly, a higher content of perfluorocarbon in the copolymer can lead to a more efficient production of reactive oxygen species, thereby improving the PDT efficiency *in vitro* (Scheme 1).

2. Experimental details

2.1 Materials

Poly(ethylene glycol)methacrylate (PEGMA, $M_n \sim 500$ g moL^{-1}) was purchased from Sigma Aldrich and used as received. 1*H*,1*H*,2*H*,2*H*-perfluorodecyl methacrylate (FDeMA), and *n*-decyl methacrylate (DEMA) was purchased from Polysciences, Inc. and used as received. 2,2′-Azobisisobutyronitrile (AIBN) was recrystallized from methanol twice and dried prior to use. Hypocrellin B (HB) dye was purchased from Beijing Fluorescence Biotech. Anhydrous toluene was purchased from Fisher (purity >99%) and used as received. Chain transfer agent was synthesized according to a previous literature.[21]

2.2 Polymer characterization

Number-average molar mass (M_n) and dispersity (M_w/M_n) of the polymers were measured by a Waters 1515 gel permeation chromatograph (GPC) with tetrahydrofuran (THF) as the eluting solvent. ^1H and ^{19}F NMR spectra were recorded on Bruker AC-400 (400 MHz) spectrometers. Acetone-d_6 was used as the solvent.

2.3 Polymer synthesis

Amphiphilic/fluorous random polymers were synthesized according to a previous literature report.[20] A typical procedure for synthesis of P(PEGMA-*co*-FDeMA) (P_5-F42%, entry 5, Table 1) random copolymer is as follows. Chain transfer agent (CTA) (6.3 mg, 0.028 mmol), PEGMA (1.05 mL, 2.28 mmol), FDeMA (0.51 mL, 1.52 mmol) and AIBN (1.45 mg, 8.83 μmol) were loaded into a Schlenk tube in a glovebox. Anhydrous toluene was used as the solvent. The Schlenk tube was sealed in the glovebox and taken out quickly and immersed in an oil bath at 70 °C. After 48 h, the Schlenk tube was submerged into liquid N_2 to quench the polymerization. Polymer solution was then precipitated into cold hexane. GPC: M_n = 30 000 g mol^{-1}, dispersity = 1.42. ^1H NMR and ^{19}F NMR results agreed well with the previous literature report.[20] Other polymers, P_1-0%, P_2-H54%, P_3-F21%, P_4-F35%, and P_6-F58%, were similarly prepared and characterized. Table 1 lists all the data.

2.4 Determination of theoretical molecular weight

The theoretical number average molar mass ($M_{n,th}$) was calculated using eqn (1)

$$M_{n,th} = \frac{[M_1]_0 \rho M_{M1} + [M_2]_0 \rho M_{M2}}{[CTA]_0 + 2f[I]_0(1 - e^{-k_d t})\left(1 - \frac{f_c}{2}\right)} + M_{CTA}$$

where $[M_x]_0$, $[I]_0$ and $[CTA]_0$ are the initial concentrations of the (co)-monomers, initiator and chain transfer agent, respectively; ρ is the monomer conversion as determined by ^1H NMR, following an average vinylic proton signal of the two co-monomers at 5.7 ppm, using pendent protons (–OC$\boldsymbol{H}_2$–) at 4.1–4.6 ppm as an internal reference, then calculating fraction of the individual co-monomer incorporated after purification to determine the individual monomer conversion. M_{M1}, M_{M2}, and M_{CTA} are the molar masses (g mol^{-1}) of the two co-monomers and chain

transfer agent, respectively. The factor "2" accounts for two radicals generated from one molecule of azoinitiator with efficiency f (assumed to be 0.5 for AIBN) to react with monomers to initiate propagating chains. The decomposition rate constant k_d has a value of 3.81×10^{-5} s^{-1}, which is calculated from the Arrhenius equation at 70 °C. Time t is polymerisation time (in seconds). The term $(1 - f_c/2)$ represents the number of chains produced in a radical–radical termination event. The coupling factor f_c has a value between 1 (100% termination occurs by bimolecular combination) and 0 (100% termination occurs by disproportionation). For simplicity, in this study, 100% termination is assumed to be by disproportionation ($f_c = 0$).

2.5 Preparation and characterization of F–polymer (P_6-F59%)–HB and H–polymer (P_2-H54%)–HB micelles

The self-assembly of polymers was adapted from a previously reported co-solvent self-assembly method.[22] Specifically, 125 mg random copolymer was first dissolved in 0.75 mL dimethylformamide (DMF) solvent for complete dissolution. Then 0.25 mL of HB dye stock solution (6.9 mg mL^{-1} in DMF) was added and the mixture was stirred for half an hour, followed by a slow addition of 2 mL deionized water (2 mL h^{-1}) and a quick addition of 7 mL of deionized water (7 mL h^{-1}) through a syringe pump. The total volume became 10 mL, with a polymer concentration of 12.5 mg mL^{-1} and the HB dye concentration of 0.173 mg mL^{-1} (free HB + loaded HB). Next, the polymer solution was dialyzed against deionized water with stirring for 3 days to remove DMF and free HB dyes.

The size of micelles was estimated by dynamic light scattering (DLS) using Zetasizer Nano S90. The optical intensities at 476 nm of ultraviolet–visible (UV-Vis) absorbance spectra were measured to determine the concentration of the loaded HB dye. The average of absorbance reading was used for calculating loading efficiency based on the Beer–Lambert law, where ε = 2900 M^{-1} cm^{-1}. Fluorescence spectra of samples were measured using a RF-5301-PC spectrofluorometer (SHIMADZU, Japan).

2.6 Detection of singlet oxygen

The singlet oxygen generation (SOG) by F–polymer–HB was determined with singlet oxygen sensor green (SOSG) as the indicator.[23] Briefly, SOSG was mixed with the F–polymer (P_6-F59%)–HB, H–polymer (P_2-H54%)–HB or HB only solutions to reach a final concentration of 1.0 μM of SOSG and HB. Specifically, free HB dye was dissolved in DMF and then diluted to 1.0 μM in water. Polymer–HB was diluted in water to 1.0 μM of HB. The working solution of SOSG was 1.0 μM, too. This dilution was necessary for measuring the singlet O_2 generation, because a higher concentration would saturate the measured fluorescence. Each sample was then irradiated with a 630 nm LED lamp (Marubeni, California, USA).[24] After the solution was irradiated for a specific time length (5, 10, 20, 30, 40, 50 and 60 min), the fluorescence emission of SOSG was measured with an RF-5301PC spectrofluorophotometer under 488 nm excitation. The sample's SOG was compared with the background or control samples.

2.7 *In vitro* cytotoxicity and measurement of PDT efficiency

The original solutions (0.163 mM of HB) prepared in Section 2.5 were too concentrated for cell study; therefore, F–polymer (P_6-F59%)–HB and H–polymer (P_2-H54%)–HB solutions were diluted in cell culture medium. The concentrations of HB in F–polymer (P_6-F59%)–HB or H–polymer (P_2-H54%)–HB were determined to be 10 000, 5000, 1000, 500 and 100 nM. As the control, HB dye only solutions with corresponding HB dye concentration to above values were also prepared. Concerning the toxicity of DMF to cells, free HB dye was first dissolved in dimethyl sulfoxide (DMSO) instead of DMF and then diluted in cell culture medium.

The H1299 cells were grown in 96-well plates (8×10^3 cells per well) overnight. H–polymer–HB, F–polymer–HB, or HB dye only (with identical amount of HB) solutions were added and incubated at 37 °C for 24 h in dark, separately. For toxicity study, cells were washed three times with PBS, and 10 μL of MTT solution (5 mg mL^{-1} MTT in PBS, pH 7.4) was then added into each well and incubated for another 4 h. After removing the medium, the wells were washed with PBS. The intracellular formazan crystals were then fully dissolved with 100 μL DMSO. The absorbance at 590 nm was measured using a plate reader. The cell viability was calculated by comparing the treated cells with untreated control. To study the *in vitro* effects of PDT, the cells were washed with PBS three times, which were immediately irradiated by 630 nm LED lamp at the dose power of 6 J per well in fresh medium. After irradiation, the cells were cultured for another 24 h. Cell viability was estimated by the standard MTT assay.

3. Results and discussion

3.1 Synthesis of perfluorocarbon-based random copolymer

In order to test our hypothesis and explore the effect of perfluorooctyl content on PDT efficacy, we designed and synthesized a series of random copolymers as shown in Scheme 2. Similar to other PFCs, perfluorooctyl has a high affinity to O_2.[25] Specifically, we synthesized amphiphilic and fluorous random copolymers P(PEGMA-*co*-FDeMA), carrying poly(ethylene glycol) chains and perfluorinated alkane pendants (*i.e.*, perfluorooctyl), through RAFT polymerization of PEGMA and FDeMA. Random copolymer P(PEGMA-*co*-FDeMA) with different amounts of FDeMA was synthesized to study how the amount of perfluorinated alkane pendants will influence the O_2 carrying ability. For comparison, control polymer without PFC, *i.e.*, homopolymer P(PEGMA), and random copolymer P(PEGMA-*co*-DeMA) (DeMA is the non-fluorinated counterpart to FDeMA) were also synthesized. The PEGMA component was to serve as a water-soluble corona to stabilize the micelles formed by P(PEGMA-*co*-FDeMA) or P(PEGMA-*co*-DeMA) in water. The feed ratio of monomers, CTA and AIBN initiator was listed in Table 1. Agreeing well with previous literature reports, all copolymerizations went smoothly, leading to designed polymers with number average molar mass ranging from 16 000 g mol^{-1} to 31 000 g mol^{-1} and relatively narrow dispersity ($Đ$) (Table 1). Successful synthesis was evidenced by ^1H and/or ^{19}F NMR (spectra in ESI,†).

Based on the NMR results, we renamed our polymers with F amount for clarity: homopolymer P(PEGMA) (entry 1 in Table 1) as P_1-0%, control polymer P(PEGMA-*co*-DeMA) (no F, entry 2 in Table 1) as P_2-H54%, and PFC-bearing polymers as P_3-F21%, P_4-F35%, P_5-F42% and P_6-F59%, respectively. The details about the polymer information are shown in Table 1. DLS results (ESI,† Fig. S2) showed that the hydrodynamic diameters of spheres (D_h) formed by P(PEGMA-*co*-FDeMA) (P_6-F59%) and P(PEGMA-*co*-DeMA) (P_2-H54%) were around 120 nm and 10 nm, respectively. We also conducted TEM to verify these sizes (Fig. S3, ESI†). These results agree well with previous reports.[20,26] The smaller size of micelle formed by the control polymer P(PEGMA-*co*-DeMA) may be due to the smaller size of DeMA side chain compared to the bulky and stiff perfluorooctyl side chain.[27]

3.2 O_2 carrying ability of pure polymers

To further prove our hypothesis, we first tested the O_2 carrying ability of the polymer synthesized. We hypothesized that the O_2 carrying ability is directly correlated to the amount of perfluorocarbon in the copolymer, *i.e.*, higher content of perfluorocarbon would help to retain the O_2 better and slow down the rate of O_2 depletion. Experimentally, we first bubbled O_2 into the solution to make it saturated with O_2. The O_2 concentration in solution was then monitored over time using an O_2 gas sensor.[28] Because of the identical experimental condition, we assume that the initial O_2 concentration in all solutions should be essentially the same, *i.e.*, saturated O_2 concentration. The concentration of O_2 in solution would then decrease with time due to the diffusion of solution O_2 into the air. Eventually, it would be equivalent to the atmospheric O_2 that can be dissolved in the solution. However, the rate of decreasing O_2 in solution would be different; the solution without PFC (for instance, P_1-0% and P_2-H54%) would show a faster rate of decreasing O_2 compared to solutions with PFC (*i.e.*, P_6-F59%). Further, polymers with more fluorine component would demonstrate higher O_2 carrying ability and thereby a slower rate of decreasing O_2.

Indeed, experimental results summarized in Fig. 1 agree well with our hypothesis. As shown in Fig. 1a, all polymer solutions have higher O_2 concentration compared to pure H_2O solvent, and solutions with PFC show higher O_2 carrying ability. Specifically, the O_2 concentration of P_1 (F conc. in solution: 0 mM), P_2-H54% (F conc. in solution: 0 mM), P_3-F21% (F conc. in solution: 5.0 mM), P_4-F35% (F conc. in solution: 8.3 mM), P_5-F42% (F conc. in solution: 10.1 mM) and P_6-F59% (F conc. in solution: 13.9 mM) is 38.36 ppm, 36.60 ppm, 35.90 ppm, 35.76 ppm, 38.33 ppm and 40.87 ppm at 1 h, respectively. These numbers decrease to 30.97 ppm, 26.22 ppm, 28.28 ppm, 29.90 ppm, 28.40 ppm and 34.80 ppm at 3.5 h; further down to 22.19 ppm, 21.76 ppm, 19.75 ppm, 21.54 ppm, 24.40 ppm and 29.60 ppm at 6 h; and finally to 9.51 ppm, 9.28 ppm, 10.67 ppm, 11.32 ppm, 9.46 ppm and 18.79 ppm at 20 h. The polymer with the highest content of PFCs (*i.e.*, P_6-F59%, F conc. in solution: 13.9 mM) can increase the O_2 carrying amount by 100% at 20 h (from 9.28 to 18.79 ppm) compared with the control polymer without any PFC (P_2-H54%). However, there is a minimum PFC conc. required for effective O_2 carrying ability. For instance, the O_2 concentration in P_5-F42% with a lower F amount (F conc. in solution: 10.1 mM) solution is almost the same with H_2O after 20 h. We further explored the influence of the amount of PFCs on the O_2 carrying ability by measuring the O_2 carrying ability of P_6-F59% (the polymer having the highest fluorine amount in this study) on the concentration of this polymer. Three different concentrations were studied, 2.5 mg mL^{-1} (F: 2.78 mM), 7.5 mg mL^{-1} (F: 8.34 mM) and 12.5 mg mL^{-1} (13.9 mM), together with the control polymer, P_2-H54% (12.5 mg mL^{-1}). Since the to-be-used HB dye has a low solubility in water, for this experiment (Fig. 1b), we prepared the polymer solution through the co-solvent assembly method described in Section 2.5 (*i.e.*, dissolve polymers in DMF first, then add H_2O slowly into the polymer solution) and removed the organic solvent through dialysis. This preparation method would mimic the preparation of the micelle incorporated with the HB dye (see Section 3.3). As shown in Fig. 1b, the O_2 carrying ability increases as the concentration of P_6-F59% increases from 2.5 to 7.5 mg mL^{-1}, and then levels off at a higher concentration of 12.5 mg mL^{-1}. Compared to the control polymer P_2-H54%, P_6-F59% can increase the O_2 concentration by 33% (from 21.65 ppm to 28.05 ppm) after 6 h. Interestingly, all formulations showed no O_2 concentration difference at the 20 h time point when the initial dissolving solvent was DMF (Fig. 1b). We believe the difference between the O_2 carrying ability at 20 h for P_6-F59% in Fig. 1a and in Fig. 1b could be caused by the different micelle preparation methods. The polymer solution in Fig. 1a was directly prepared by dissolving the polymer in H_2O while the polymer solution in Fig. 1b was made from a co-solvent based self-assembly method. There might be some subtle difference in the structure and morphology of micelles prepared with different methods, which would lead to the

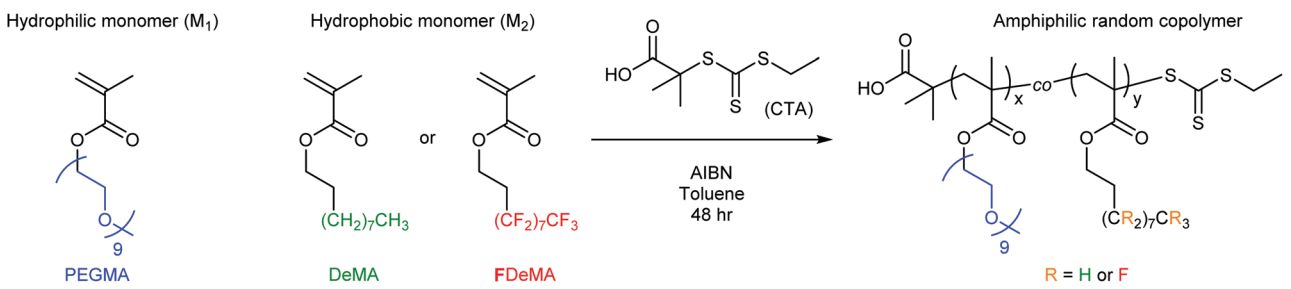

Scheme 2 Synthesis of amphiphilic/fluorous random copolymers.

Table 1 Details of polymerization and polymers in this work

Entry	$[M_1]:[M_2]:[CTA]:[I]^a$	Conv.^{b} (%)	Final polymer composition^c	$M_{n,th}{}^d$ (g mol^{-1})	$M_{n,GPC}{}^e$ (g mol^{-1})	$Đ^d$	M_2 (%)	Name
1	150 : 0 : 1 : 0.26	93	P(PEGMA$_{140}$)	56 000	16 000	1.24	0	P$_1$-0%
2	72 : 72 : 1 : 0.26	90	P(PEGMA$_{59}$-*co*-DeMA$_{70}$)	36 000	27 000	1.32	54	P$_2$-H54%
3	120 : 30 : 1 : 0.26	93	P(PEGMA$_{110}$-*co*-FDeMA$_{29}$)	56 000	25 000	1.28	21	P$_3$-F21%
4	105 : 45 : 1 : 0.26	93	P(PEGMA$_{96}$-*co*-FDeMA$_{43}$)	57 000	31 000	1.38	35	P$_4$-F35%
5	86 : 57 : 1 : 0.26	90	P(PEGMA$_{74}$-*co*-FDeMA$_{54}$)	53 000	30 000	1.42	42	P$_5$-F42%
6	72 : 72 : 1 : 0.26	67	P(PEGMA$_{39}$-*co*-FDeMA$_{57}$)	40 000	28 000	1.39	59	P$_6$-F59%

^{a} Initial monomer feed ratio, where M_1 is the hydrophilic monomer (PEGMA) and M_2 is the hydrophobic monomer either non-fluorinated (DeMA) or fluorinated (FDeMA). ^{b} Average co-monomer conversion determined experimentally by NMR ($CDCl_3$), following the vinylic protons at 5.7 ppm using pendent protons (–OC***H***$_2$–) at 4.1–4.6 ppm as an internal reference. ^{c} Final composition and molar percentage of M_2 were determined by NMR after purification, methoxy –OC***H***$_3$ protons at 3.5 ppm were used to evaluate the incorporation of PEGMA (M_1) within a region representing both co-monomers (–OC***H***$_2$–) at 4.1–4.6 ppm, also taking into consideration the average co-monomer conversion. ^{d} Theoretical molar mass ($M_{n,th}$) was determined from eqn (1). ^{e} Experimental molar mass ($M_{n,SEC}$) and dispersity ($Đ$) were obtained from gel permeation chromatography analysis with THF as the eluent and polystyrene as calibration standards.

observed difference at longer time scales (20 h). Nevertheless, the oxygen carrying capability was not affected at early time points (*e.g.*, P$_6$-F59% at 12.5 mg mL^{-1} within 6 hours) regardless of whether the initial dissolving solvent was H_2O or DMF. In order to incorporate the water-insoluble hypocrellin B (HB) photosensitizer into the core of polymer micelle, we chose DMF as the initial dissolving solvent in subsequent experiments. Because of its highest O_2 carrying ability, we chose P$_6$-F59% for further study. P$_2$-H54% was also studied as the reference.

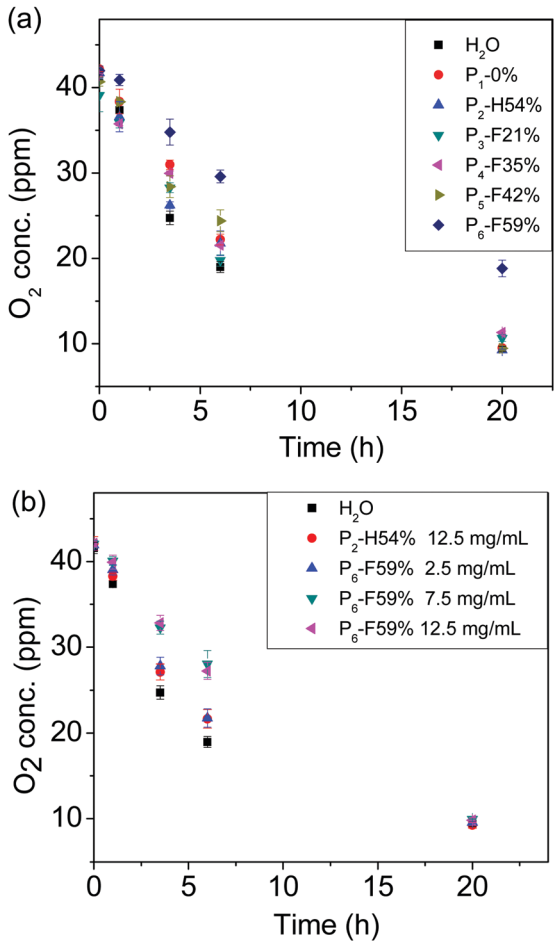

Fig. 1 (a) O_2 carrying ability of various polymers with concentration 12.5 mg mL^{-1} in H_2O and (b) O_2 carrying ability of P$_6$-F59% with different polymer concentrations ranging from 2.5 mg mL^{-1} to 12.5 mg mL^{-1} after dialysis.

These micelles seem to be quite robust; Fig. S4 and S5 in ESI,† demonstrate that neither pH nor encapsulation of the HB dye would affect the oxygen carrying ability and increased temperature would slightly reduce the oxygen concentration in the solution in all time points, which may be due to the faster diffusion rate of oxygen in the solution at higher temperatures.

3.3 UV-Vis spectra and fluorescence spectra of HB dye incorporated micelles

We chose hypocrellin B (HB),[29] a photosensitizer for PDT, in this study. HB dye was incorporated into the copolymer through the co-solvent self-assembly method described in Section 2.5. As shown in Fig. S2 (ESI†) in the supporting information, the micelle size increased from 120 nm to 200 nm after the incorporation of HB dye into the P$_6$-F59%. Through measuring the absorbance of the HB dye and comparing to standard HB dye UV-Vis absorption curve, we determined the actual amount of HB dye incorporated into the micelles as 0.0862 mg mL^{-1} (0.163 mM). The loading efficiency was then calculated to be (0.0862 mg/0.173 mg) × 100% = 49.9%. The ratio of polymer : HB was (12.5 : 0.0862) = 145 : 1.

In order to make the PDT results comparable among different groups in our study, we kept the amount of photosensitizer identical in all groups. As shown in Fig. 2, F–polymer (*i.e.*, P$_6$-F59%)–HB, H–polymer (*i.e.*, P$_2$-H54%)–HB and HB stock solutions show almost identical absorbance at 470 nm (where the HB dye absorption maximum is), indicating that a comparable amount of HB was dissolved or encapsulated in solution/micelle for each group. The fluorescence spectra of F–polymer–HB, H–polymer–HB and free HB were next compared to discern any changes in the photophysical and photochemical properties of the HB dye after the incorporation. We observed almost identical fluorescence intensity at 625 nm for both F–polymer (*i.e.*, P$_6$-F59%)–HB and H–polymer (*i.e.*, P$_2$-H54%)–HB. This further proves that a comparable amount of HB dye was incorporated into the micelle for each group. However, the fluorescence of pure HB in water is very low. This low fluorescence is likely due to its low solubility in water, causing aggregation induced

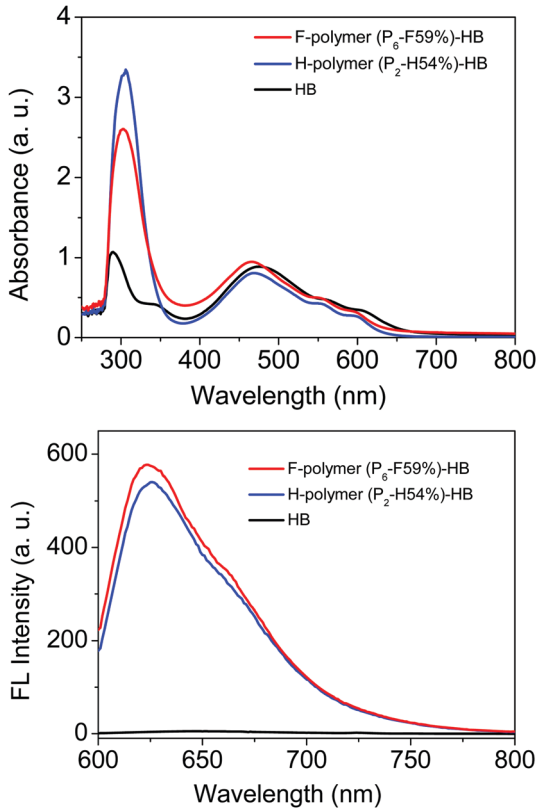

Fig. 2 UV-Vis and fluorescence spectra of HB, F–polymer (P_6-F59%)–HB and H–polymer (P_2-H54%)–HB.

quenching (AIQ). Indeed, a low quantum yield of the HB dye in water, 0.004 (*versus* 0.08 in DMSO), has been reported.[30]

3.4 Singlet O_2 measurement

Having proven the successful incorporation of HB dye into these micelles, we further measured the efficiency of $^1O_2$ production in these micelles formed with F–polymer (*i.e.*, P_6-F59%)–HB, H–polymer (*i.e.*, P_2-H54%)–HB. HB alone was tested as the control. Samples were prepared according to Section 2.6. The way to measure the $^1O_2$ production was adapted from a previous literature report.[23] Considering that a longer wavelength will have a longer penetration length, we chose 630 nm as the wavelength for our experiments, similar to previously reported *in vivo* experiments.[24] We measured the $^1O_2$ production by the green fluorescence intensity of oxidized SOSG (an indicator of $^1O_2$). A higher intensity of SOSG would indicate a higher amount of $^1O_2$. The results are shown in Fig. 3. The accumulated fluorescence intensity of SOSG exhibits a time-dependent enhancement. After these photosensitizers and the SOSG were mixed and irradiated for 60 min (630 nm,

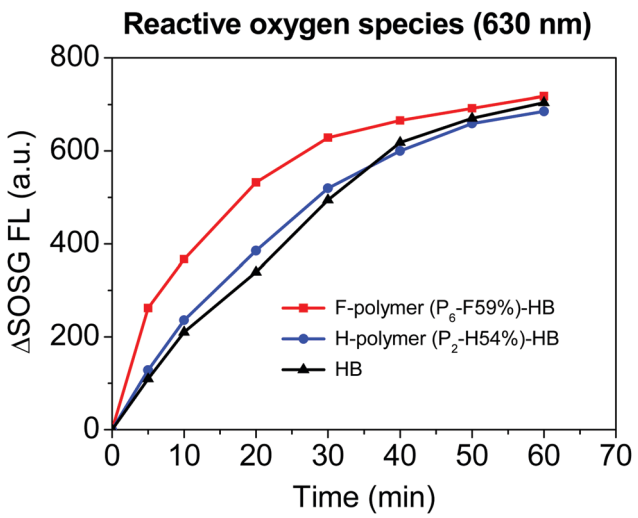

Fig. 3 $^1O_2$ production of HB, F–polymer (P_6-F59%)–HB and H–polymer (P_2-H54%)–HB under 630 nm irradiation as determined by the accumulated fluorescence intensity of oxidized SOSG.

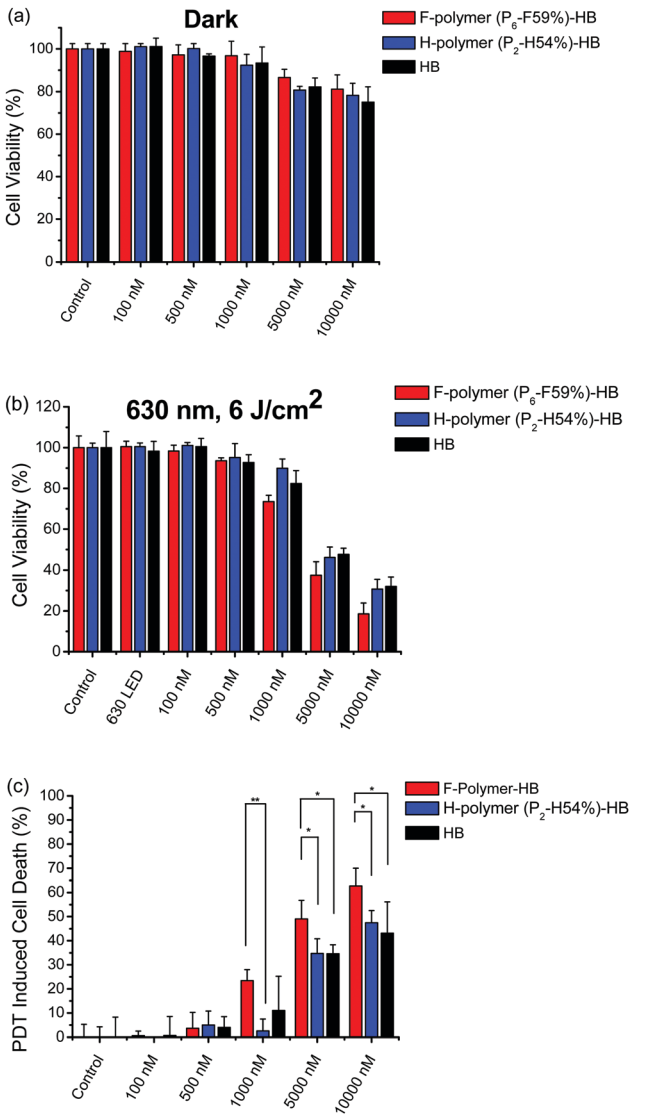

Fig. 4 (a) Cytotoxicity, (b) phototoxicity and (c) PDT induced cell death of HB, F–polymer (P_6-F59%)–HB and H–polymer (P_2-H54%)–HB against H-1299 cells in darkness and irradiation upon 630 nm, 6 J cm^{-2}. Note: the power of the lamp is 20 mW cm^{-2}, however, for a total of 300 seconds, *i.e.*, (20 mW cm^{-2} = 0.02 J (s^{-1} cm^{-2}), 0.02 J (s^{-1} cm^{-2}) × 300 s = 6 J cm^{-2}).

20 mW cm^{-2}), F–polymer (P_6-F59%)–HB demonstrated higher production of $^1O_2$ at early time points. This further proves that the incorporation of PFC effectively promotes the production of $^1O_2$. This result agrees well with previous results that PFC can carry more O_2 than hydrocarbon polymer.[25] Meanwhile, the singlet oxygen generation of H–polymer (P_2-H54%)–HB is on the same level as HB dye. We note that the data gradually reach a plateau after 40 min, which might be caused by the depletion of the limited amount of SOSG.

3.5 Characterization of photodynamic efficiency

To explore the photodynamic efficiency *in vitro*, we evaluated the photocytotoxicity of micelles of F–polymer (P_6-F59%)–HB, H–polymer (P_2-H54%)–HB and HB only on H-1299 cells. Samples were prepared according to Section 2.7. As shown in Fig. 4a, all three samples showed non-toxicity up to 1000 nM of HB when kept in the dark, indicating excellent biocompatibility. However, all three groups showed dose-dependent toxicity to cells when the concentration of HB went higher than 5000 nM. The cell viability decreased to 75.1% at the concentration of 10 000 nM of HB. Fig. 4b studied the toxicity of F–polymer–HB, H–polymer–HB and HB system under light irradiation. With a total 6 J cm^{-2} light irradiation (20 mW cm^{-2} for 300 seconds), F–polymer–HB demonstrated significantly better PDT efficacy than H–polymer–HB and HB, when HB concentration reached 1000 nM or higher. The cell viability dropped to 18.5% with light irradiation compared to 81.3% without irradiation in F–polymer–HB group with HB concentration at 10 000 nM. In other words, the light induced cell death is about 62.8% in the case of F–polymer–HB, compared with 45.4% in H–polymer–HB group and 43.2% in HB group with HB concentration at 10 000 nM, as shown in Fig. 4c. The reduction in cell viability is significantly higher in cells treated with F–polymer–HB than those treated with H–polymer–HB and HB alone (Fig. 4c, $*P < 0.05$, $**P < 0.001$). This higher cytotoxicity of F–polymer–HB can be ascribed to the much improved O_2 carrying ability and higher $^1O_2$ production of the F–polymer (*i.e.*, P_6-F59%).

4. Conclusions

In summary, we prepared a series of polymers with different perfluorocarbon components in the core. This new formulation not only enhances O_2 carrying ability of polymers, but also improves the efficacy of $^1O_2$ generation. In our initial *in vitro* evaluation, the synthesized PFC-containing polymer demonstrated lower cytotoxicity and enhanced PDT efficiency towards H-1299 cells. Although systematic *in vivo* evaluation is still needed for tumor treatment in animal models, our results presented in this work demonstrate initial success of improving PDT efficiency through our PFC-incorporated nanoplatform.

Conflicts of interest

There are no conflicts of interest to declare.

Acknowledgements

This work was financially supported by the University of North Carolina at Chapel Hill.

Notes and references

1 P. Agostinis, K. Berg, K. A. Cengel, T. H. Foster, A. W. Girotti, S. O. Gollnick, S. M. Hahn, M. R. Hamblin, A. Juzeniene, D. Kessel, M. Korbelik, J. Moan, P. Mroz, D. Nowis, J. Piette, B. C. Wilson and J. Golab, *Ca-Cancer J. Clin.*, 2011, **61**, 250–281.
2 G. Tegos, T. Dai, B. B. Fuchs, J. J. Coleman, R. A. Prates, C. Astrakas, T. G. S. Denis, M. S. Ribeiro, E. Mylonakis and M. R. Hamblin, *Front. Microbiol.*, 2012, **3**, 120.
3 T. Dai, B. B. Fuchs, J. J. Coleman, R. A. Prates, C. Astrakas, T. G. S. Denis, M. S. Ribeiro, E. Mylonakis, M. R. Hamblin and G. P. Tegos, *Front. Microbiol.*, 2012, **3**, 120.
4 P. Prasad, C. R. Gordijo, A. Z. Abbasi, A. Maeda, A. Ip, A. M. Rauth, R. S. DaCosta and X. Y. Wu, *ACS Nano*, 2014, **8**, 3202–3212.
5 W. Fan, W. Bu, B. Shen, Q. He, Z. Cui, Y. Liu, X. Zheng, K. Zhao and J. Shi, *Adv. Mater.*, 2015, **27**, 4155–4161.
6 J. Kim, H. R. Cho, H. Jeon, D. Kim, C. Song, N. Lee, S. H. Choi and T. Hyeon, *J. Am. Chem. Soc.*, 2017, **139**, 10992–10995.
7 H. Chen, J. Tian, W. He and Z. Guo, *J. Am. Chem. Soc.*, 2015, **137**, 1539–1547.
8 Z. Yuan, S. Yu, F. Cao, Z. Mao, C. Gao and J. Ling, *Polym. Chem.*, 2018, **9**, 2124–2133.
9 J. D. Wallat, K. S. Wek, P. L. Chariou, B. L. Carpenter, R. A. Ghiladi, N. F. Steinmetz and J. K. Pokorski, *Polym. Chem.*, 2017, **8**, 3195–3202.
10 J. G. Riess, *Artif. Cells, Blood Substitutes, Biotechnol.*, 2005, **33**, 47–63.
11 R. Díaz-López, N. Tsapis and E. Fattal, *Pharm. Res.*, 2009, **27**, 1.
12 K. C. Lowe, *Artif. Cells, Blood Substitutes, Biotechnol.*, 2000, **28**, 25–38.
13 D. R. Spahn, *Crit. Care*, 1999, **3**, R93–R97.
14 Y. Cheng, H. Cheng, C. Jiang, X. Qiu, K. Wang, W. Huan, A. Yuan, J. Wu and Y. Hu, *Nat. Commun.*, 2015, **6**, 8785.
15 X. Song, L. Feng, C. Liang, K. Yang and Z. Liu, *Nano Lett.*, 2016, **16**, 6145–6153.
16 Y. Patil, S. Almahdali, K. B. Vu, G. Zapsas, N. Hadjichristidis and V. O. Rodionov, *Polym. Chem.*, 2017, **8**, 4322–4326.
17 C. V. Synatschke, T. Nomoto, H. Cabral, M. Förtsch, K. Toh, Y. Matsumoto, K. Miyazaki, A. Hanisch, F. H. Schacher, A. Kishimura, N. Nishiyama, A. H. E. Müller and K. Kataoka, *ACS Nano*, 2014, **8**, 1161–1172.
18 W. L. Kim, H. Cho, L. Li, H. C. Kang and K. M. Huh, *Biomacromolecules*, 2014, **15**, 2224–2234.
19 Y. Que, Y. Liu, W. Tan, C. Feng, P. Shi, Y. Li and H. Xiaoyu, *ACS Macro Lett.*, 2016, **5**, 168–173.
20 Y. Koda, T. Terashima, M. Sawamoto and H. D. Maynard, *Polym. Chem.*, 2015, **6**, 240–247.

21 A. J. Convertine, B. S. Lokitz, Y. Vasileva, L. J. Myrick, C. W. Scales, A. B. Lowe and C. L. McCormick, *Macromolecules*, 2006, **39**, 1724–1730.
22 G. Gaucher, M.-H. Dufresne, V. P. Sant, N. Kang, D. Maysinger and J.-C. Leroux, *J. Controlled Release*, 2005, **109**, 169–188.
23 H. Lin, Y. Shen, D. Chen, L. Lin, B. C. Wilson, B. Li and S. Xie, *J. Fluoresc.*, 2013, **23**, 41–47.
24 J.-E. Chang, H.-J. Cho, E. Yi, D.-D. Kim and S. Jheon, *J. Photochem. Photobiol., B*, 2016, **158**, 113–121.
25 D. R. Spahn, *Adv. Drug Delivery Rev.*, 2000, **40**, 143–151.
26 G. Hattori, Y. Hirai, M. Sawamoto and T. Terashima, *Polym. Chem.*, 2017, **8**, 7248–7259.
27 J. G. Riess, *Curr. Opin. Colloid Interface Sci.*, 2009, **14**, 294–304.
28 R. Ramamoorthy, P. K. Dutta and S. A. Akbar, *J. Mater. Sci.*, 2003, **38**, 4271–4282.
29 G. G. Miller, K. Brown, Å. M. Ballangrud, O. Barajas, Z. Xiao, J. Tulip, J. W. Lown, J. M. Leithoff, M. J. Allalunis-Turner, R. D. Mehta and R. B. Moore, *Photochem. Photobiol.*, 1997, **65**, 714–722.
30 B. Zhao, J. Xie and J. Zhao, *Biochimica et Biophysica Acta*, 2005, **1722**, 124–130.